

Manipulating 4f quadrupolar interactions in TbB_2C_2 by a magnetic field

A.M. Mulders¹, U. Staub¹, V. Scagnoli¹, Y. Tanaka², A. Kikkawa², K. Katsumata² and J.M. Tonnerre³

¹*Swiss Light Source, Paul Scherrer Institut, 5232 Villigen PSI, Switzerland*

²*RIKEN SPring-8 Center, Harima Institute, Sayo, Hyogo 679-5148, Japan and*

³*CNRS Grenoble, 38042 Grenoble Cedex 9, France*

(Dated: December 2, 2024)

Resonant soft x-ray Bragg diffraction at the Tb $M_{4,5}$ edges and non resonant Bragg diffraction have been used to investigate orbital motifs in TbB_2C_2 . The Tb 4f quadrupole moments are ordered in zero field below T_N in contrast to the earlier suggestions and show a ferroquadrupolar alignment dictated by the antiferromagnetic order. With increasing applied field along [110] the Tb 4f magnetic dipole moments rotate in a gradual manner toward the field direction. The orbital moment is rigidly coupled to the magnetic moment and follows this field-induced rotation. While the exchange interaction between spins does not depend much on their orientation, the orbital interaction is found to depend on the specific orientation of the orbitals and can be manipulated with an applied field.

PACS numbers: 71.70.Ch; 75.40.Cx; 78.70.Ck

Correlation between conduction electrons and electronic orbitals leads to interesting material properties such as metal-insulator transitions, colossal magneto resistance and superconductivity. Aspheric electronic orbitals, characterized by their quadrupole moment, may order in specific motifs and cause partial charge localization of the conduction electrons¹ or mediate coupling between cooper pairs.² Although orbital ordering has been studied in detail in *f*-electron materials³ little is known concerning the interaction between the quadrupole moments because of the difficulty to observe orbital excitations. Yet, the large orbital momentum of the *f* electronic shell gives rise to significant influence of higher multipole moments and this may lead to hidden order phase transitions as exemplified in the extensively studied compound URu_2Si_2 .⁴ Consequently it is important to understand what defines the interaction between the quadrupolar and higher order multipole moments.

TbB_2C_2 is a very interesting candidate to investigate orbital interactions as it is proposed to exhibit a transition from antiferromagnetic (AFM) to antiferroquadrupolar (AFQ) order in applied magnetic field. A magnetic field is time-odd and cannot couple to quadrupole moment which is time-even, but nevertheless the ordering temperature increases to 35 K, well above $T_N = 21.7$ K, in applied magnetic field of 10 T.⁵ This makes TbB_2C_2 an ideal compound in which to investigate the interplay between dipole (time-odd) and quadrupole (time-even) moments.

Recently the direct observation of orbital motifs has been achieved with the use of x-ray diffraction. Resonant x-ray scattering at the $L_{2,3}$ edge provided the first proof of the orbital motif in DyB_2C_2 .^{6,7} A recent resonant scattering study at the $M_{4,5}$ edge determined high-order multipole moments.⁸ In addition, the orbital fluctuation time has been determined from neutron scattering.⁹ The orbital interaction dominates the 4f magnetic exchange interaction in DyB_2C_2 . A structural transition at the AFQ ordering temperature, T_Q , is evidenced by alter-

nating displacements of B and C atoms along the *c*-axis and is proposed to cooperate with the AFQ order.

The occurrence of AFQ order under applied magnetic fields in TbB_2C_2 has been proposed from magnetisation measurements.⁵ Neutron diffraction studies revealed similarities between the magnetic structure in applied fields and the magnetic structure in the combined AFQ and AFM phase of DyB_2C_2 .¹¹ However, resonant x-ray diffraction at the Tb L_3 edge suggests AFQ is present below T_N in zero field with a *k* vector component of $(0,0,\frac{1}{2})$ as for DyB_2C_2 .¹²

To test the suggested field-induced orbital ordering we investigate TbB_2C_2 in an applied magnetic field, H , with x-ray scattering techniques. We establish the role of the quadrupolar interaction and show that orbital order is present in the AFM phase of TbB_2C_2 at zero field, however, with ferroquadrupolar alignment which is dictated by the AFM structure. Moreover, the quadrupoles rotate with H along the [110] direction and are rigidly linked to the magnetic dipole moments. Due to this rotation the AFQ interaction becomes stronger with applied field.

A TbB_2C_2 single crystal has been grown by Czochralski method using an arc-furnace with four electrodes. Samples have been cut and polished perpendicular to the [001] direction. The $(00\frac{1}{2})$ reflection has been recorded at the Tb $M_{4,5}$ edges of TbB_2C_2 at the RESOXS end-station of the SIM beamline at the Swiss Light Source of the Paul Scherrer Institut. A permanent magnet provides a field of 1 T parallel to the [110] direction in the scattering plane. In addition, non resonant x-ray Bragg diffraction at $(01\frac{1}{2})$ and $(11\frac{1}{2})$ reflections has been performed at the BL19LXU beam line at SPring-8 with 30 keV x-rays with a Ge solid-state detector to eliminate higher order harmonics. A cryomagnet provides H along the [110] direction. In both sets of measurements, structure factors were derived from the integrated intensity, corrected for polarization, Lorenz factor, absorption and sample geometry.

Figure 1a shows the energy dependence of the $(00\frac{1}{2})$ re-

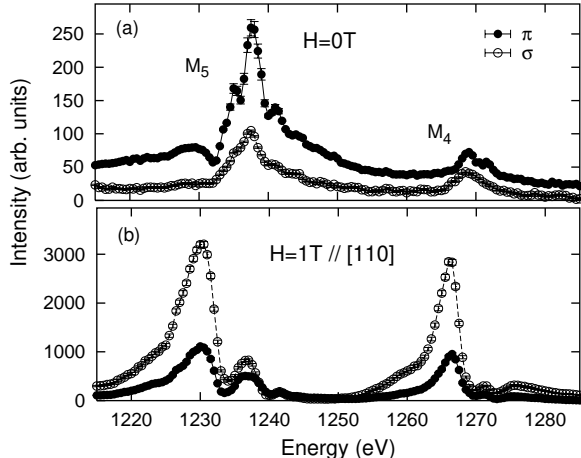


FIG. 1: Energy profile of the $(00\frac{1}{2})$ reflection at the Tb $M_{4,5}$ edges in TbB_2C_2 in (a) zero field and (b) applied field of 1 T along [110], recorded with σ or π incident radiation at 11 K.

lection recorded at the Tb $M_{4,5}$ edges in zero field. The energy profile is independent of sample rotation about the Bragg wave vector. Significant part of the diffracted intensity is due to total reflectivity of the polished sample. The $(00\frac{1}{2})$ diffracted intensity is relatively weak and appears magnetic of origin as witnessed by the relatively large intensity for incoming x-rays polarized in the scattering plane (π). In contrast, the diffracted intensity with $H = 1$ T, along the [110] direction, shown in Fig. 1b is much stronger and strongest for incoming radiation polarized perpendicular to the scattering plane (σ). The energy profiles shown in Fig. 1 are expected to be insensitive to the magnetic structure, not to be confused with the total intensity that does depend on the magnetic order. The observed change with H indicates the presence of either an additional component of resonant scattering or a change in relative contribution of two different components of resonant scattering. The energy profile recorded with applied magnetic field is similar to that recorded for the $(00\frac{1}{2})$ reflection in DyB_2C_2 in the AFQ phase.¹³ This implies that in TbB_2C_2 the $(00\frac{1}{2})$ reflection is dominated by orbital scattering under an applied magnetic field of 1 T.

Fig. 2a,b shows the structure factors, obtained from the integrated, non-resonant Bragg intensities of the $(01\frac{9}{2})$ and $(11\frac{15}{2})$ reflection as a function of applied field, that relate directly to the order parameter. In the AFM phase, at 15 K, the structure factors show a linear increase for applied fields below 1.5 T. In the paramagnetic phase, at 27 K, the ordered phase is entered above 3 T. Remarkably, the $(01\frac{9}{2})$ reflection appears at 3.2 T while the $(11\frac{15}{2})$ reflection appears at 3.5 T. Nevertheless, the evolution of the structure factor with field is smooth for both reflections without a hint of a phase transition at 3.5 T for $(01\frac{9}{2})$. A similar behavior is observed as function of temperature in an applied field of 5 T (not shown). The intensity at $(01\frac{9}{2})$ and $(11\frac{15}{2})$ shows a smooth decrease with increasing temperature and disappears below 30 K and 29.5 K, respectively.

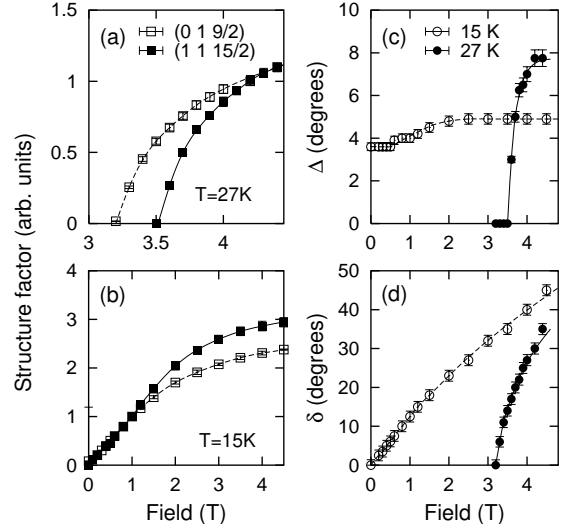


FIG. 2: Structure factor of the $(01\frac{9}{2})$ and $(11\frac{15}{2})$ reflection as function of applied magnetic field recorded with 30 keV at (a) $T = 27$ K and (b) $T = 15$ K. (c) and (d) show the deduced angles of Tb $4f$ orbital rotation as defined in Fig. 3.

A structural transition with alternating displacements of the B and C atoms gives intensity in both type of reflections¹⁴ and cannot account for the present observation of intensity at $(01\frac{9}{2})$ and the absence of intensity at $(11\frac{15}{2})$. Magnetic, or time-odd, x-ray diffraction is weak and cannot explain the observed magnitude of intensity. In contrast, scattering from aspheric charge distribution of the $4f$ shell, time-even x-ray diffraction, can be intense. Therefore we explore a time-even origin of these reflections.

It is assumed that the Tb ion on each site has the same charge distribution except for its specific orientation. Using the formalism for non resonant time-even scattering of Lovesey *et. al.*¹⁵ we deduce two independent Tb ions contribute and obtain for the structure factors:

$$F_{11\frac{1}{2}} \propto -2 [\sin(2\phi_1) - \sin(2\phi_3)] \langle Q_{11\frac{1}{2}} \rangle, \quad (1)$$

$$F_{01\frac{1}{2}} \propto [\cos(2\phi_1) - \cos(2\phi_3)] \langle Q_{01\frac{1}{2}} \rangle, \quad (2)$$

where the Miller index l equals an odd integer. The principal axis of the $4f$ orbital at atom n is canted in the ab -plane with respect to the [100] direction with angle ϕ_n . $\langle Q_{hkl} \rangle$ is the expectation value of the Tb $4f$ time-even multipolar moment for a given field, temperature and Bragg wave vector $\mathbf{k} = (k_a, k_b, k_c)$:

$$\langle Q_{11\frac{1}{2}} \rangle \propto \frac{k_b^2}{k^2} \left[\langle j_2 \rangle \Psi_2^2 + 3\sqrt{3} \langle j_4 \rangle \Psi_2^4 - \sqrt{182} \langle j_6 \rangle \Psi_2^6 \right], \quad (3)$$

$$\langle Q_{01\frac{1}{2}} \rangle \propto \langle Q_{11\frac{1}{2}} \rangle + \frac{k_b^2}{k^2} \sqrt{21} \langle j_4 \rangle \Psi_4^4. \quad (4)$$

Ψ_q^x is a structure factor of the chemical unit cell that is a linear sum of atomic tensors, $\Psi_q^x = \langle T_q^x \rangle - \langle T_{-q}^x \rangle$. $\langle T_q^x \rangle$ describes the asphericity of the Tb $4f$ electronic shell where $\langle T_2^2 \rangle$ equals the quadrupole moment, $\langle T_2^4 \rangle$ the hexadecapole moment and $\langle T_2^6 \rangle$ the hexacontatetrapole moment. $\langle j_2 \rangle$, $\langle j_4 \rangle$ and $\langle j_6 \rangle$ are Bessel function transforms

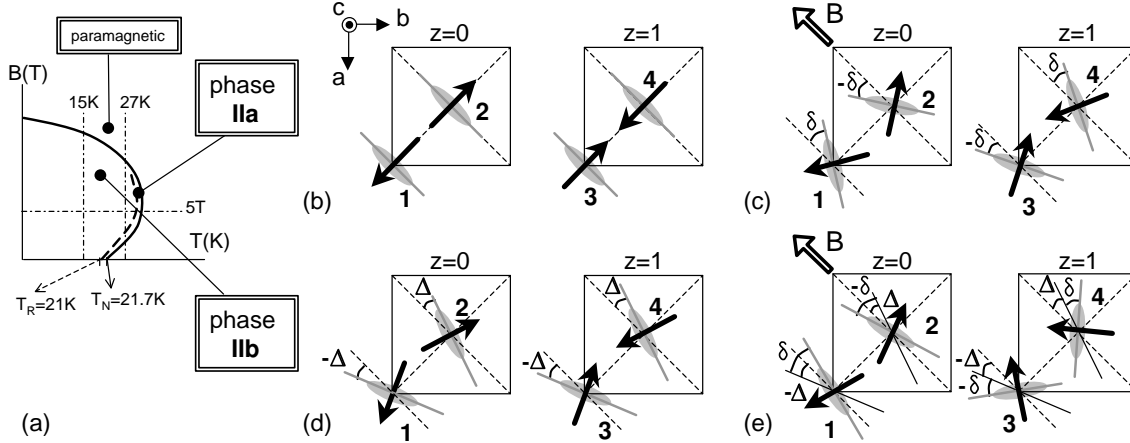


FIG. 3: (a) Phase diagram of TbB_2C_2 with magnetic field applied along $[110]$. (b) and (c) illustrate the orientation of magnetic moments (arrows) and quadrupole moments (ovals) in TbB_2C_2 in phase IIa in zero field and under applied fields, respectively. (d) and (e) illustrate phase IIb under the same conditions.

of the radial distribution of the $4f$ electronic charge. In eqs. 3 and 4, $(k_c/k)^2 \sim 1$ and we neglect higher order terms $(k_b/k)^4$ and $(k_b/k)^6$ as $k_b/k \ll 1$.

We now discuss the relationship between the multipolar motif and $F_{01\frac{1}{2}}$ and $F_{11\frac{1}{2}}$. When the $4f$ quadrupoles are aligned along $[110]$ ($\phi_1 = \phi_3 = \frac{3}{4}\pi$) as drawn in Fig. 3(b), $F_{01\frac{1}{2}}$ and $F_{11\frac{1}{2}}$ are both zero. When the $4f$ quadrupoles tilt toward the applied field with angle δ ($\phi_1 = \frac{3}{4}\pi + \delta$; $\phi_3 = \frac{3}{4}\pi - \delta$) as is drawn in Fig. 3(c), $F_{01\frac{1}{2}}$ is finite and $F_{11\frac{1}{2}}$ remains zero. Neutron diffraction has shown that in the AFM phase the dipole moments tilt away from $\langle 110 \rangle$ with angle Δ as illustrated in Fig. 3(d) ($\phi_1 = \frac{3}{4}\pi - \Delta$; $\phi_3 = \frac{3}{4}\pi - \Delta$).¹⁶ In this case, both $F_{01\frac{1}{2}}$ and $F_{11\frac{1}{2}}$ are zero in zero field while under an applied field both become finite (Fig. 3(e), $\phi_1 = \frac{3}{4}\pi - \Delta + \delta$; $\phi_3 = \frac{3}{4}\pi - \Delta - \delta$).

Multipole moment rotation in an applied field is linear for small δ , Δ (see Eq. (1)) which results in the linear increase of the structure factor as observed at 15 K (see Fig. 2(b)). The magnetic moment of the $4f$ shell tilts toward the direction of the magnetic field and the time-even multipole moments follow accordingly. The latter give the observed contrast. This shows that (i) the coupling between magnetic and orbital moment is rigid and (ii) the orbitals are already ordered in zero field, though with a ferroquadrupolar alignment. This is consistent with the result in Fig. 1a as ferroquadrupolar alignment in zero field does not contribute to scattering at $(00\frac{1}{2})$, whereas in an applied field, due to the orbital rotation, time-even scattering dominates (Fig. 1b).

The results from non resonant Bragg diffraction give further information. At 27 K, between $H = 3.2$ and $H = 3.5$ T, the magnetic and orbital structure of TbB_2C_2 is characterized by phase IIa. The orbitals are aligned parallel to $[110]$ as illustrated in Fig. 3(b) and are tilted in applied field as illustrated in Fig. 3(c). Above 3.5 T the compound is characterized by phase IIb. The orbitals are tilted away from the $[110]$ direction and neighboring atoms in the ab -plane are tilted in opposite directions

as illustrated for $H = 0$ in Fig. 3(d) and for $H \neq 0$ in Fig. 3(e). We show schematically the phase diagram (Fig. 3(a)) and define a reorientation temperature T_R by the boundary between phases IIa and IIb.

The normalized structure factor of $(01\frac{1}{2})$ and $(11\frac{1}{2})$ reflections at 5 T with $9 \leq l \leq 17$ and are presented in Fig 4. The k dependence is equal within the experimental uncertainty which shows that Ψ_4^4 is small (Eqs. 3 and 4). The solid line corresponds to Eqs. 1 and 3 with $\Psi_2^4/\Psi_2^2 = 0.5$ and $\Psi_2^6/\Psi_2^2 = 0.5$ and shows that the intensity can be attributed to time-even x-ray diffraction. The limited range of k makes the determination of Ψ_2^2 uncertain and this analysis merely confirms the absence of scattering from B and C atoms in contrast to DyB_2C_2 .¹⁴ Thus orbital order is present independent from a structural transition in TbB_2C_2 .

With $\langle Q_{01\frac{1}{2}} \rangle = \langle Q_{11\frac{1}{2}} \rangle$ for given field and temperature the angle Δ is deduced from the ratio between $F_{01\frac{9}{2}}$ and $F_{11\frac{15}{2}}$. In addition the quantity $\sin(2\delta)\langle Q_{hkl} \rangle$ follows from Eqs. 1 and 2 and δ has been estimated assuming $\langle Q_{hkl} \rangle$ is constant as function of field and temperature. Both results are presented in Figs. 2(c) and (d). If $\langle Q_{hkl} \rangle$ increases with H the actual values for δ are lower than presented in Fig. 2d. Nevertheless, the increase in δ is gradual as function of the applied field and reflects the orbital moment rotation. The magnitude of Δ can be interpreted as a relative strength of the AFQ interaction with respect to the magnetic exchange interaction between neighboring atoms in the ab -plane. The first interaction favors perpendicular alignment of the orbitals while the latter favors a parallel alignment. A small increase in Δ is observed with H . This shows that the relative strength of the AFQ interaction increases as the orbitals rotate perpendicular to each other in an applied field. Possibly, the increase in Δ as observed around 1 T at 15 K has been mistaken as a phase boundary in the magnetization measurements.⁵

The increase in ordering temperature with applied field⁵ is in line with an antiferroquadrupolar interaction

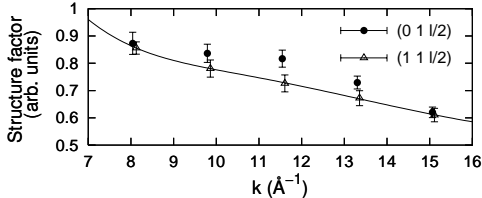


FIG. 4: Structure factor of $(01\frac{1}{2})$ and $(11\frac{1}{2})$ reflections at $B=5$ T and $T=2$ K. The solid line is a fit to Eq. 1.

which becomes stronger when the angle between the orbitals moves from parallel to perpendicular alignment. Both the magnetic exchange and orbital interactions are believed to be mediated via the conduction electrons.⁹ The magnetic moments interact via the polarized spins of the conduction electrons while the multipolar moments interact via the charge density of the conduction electrons. In other words, charge screening by the conduction electrons changes when the $4f$ orbitals rotate and consequently the magnitude of the quadrupolar interaction changes. This is in contrast to the magnetic exchange interaction which does not depend much on the moment orientation.

In DyB_2C_2 orbital order with perpendicular alignment of neighboring $4f$ orbitals along $[001]$ coexists with movement of B and C ions. In TbB_2C_2 the magnetic interaction dominates, the orbitals are aligned parallel along $[001]$ and we find no experimental evidence for B and C movement. This suggests that the orbital interaction drives the structural transition in DyB_2C_2 while in TbB_2C_2 the orbital interaction is not strong enough to drive perpendicular alignment of the $4f$ orbitals along c nor an associated structural transition.

The occurrence of combined AFQ and AFM below T_N

is consistent with the quasi doublet ground-state.¹⁷ Removal of the degeneracy of a doublet ground-state may account for one phase transition. Relaxation between the two singlets takes place above T_N and the magnetic and quadrupolar moments fluctuate. The increased energy separation between the two singlets below T_N is due to the magnetic exchange interaction but both the magnetic and quadrupolar moment of the ground state singlet are observed as illustrated by this study. The influence of the AFQ interaction is observed below T_R when the orbitals move away from $[110]$ with angle Δ .

In conclusion, no magnetic field induced ordering of orbitals exists in TbB_2C_2 . The orbitals are already ordered in the AFM phase in zero field with a ferroquadrupolar motif. On increasing the applied field along $[110]$ the Tb $4f$ magnetic moments rotate toward the field direction in a gradual manner. The orbital moment is rigidly coupled to the magnetic moment and follows this rotation. Neighboring Tb $4f$ orbitals move from parallel to perpendicular alignment and the orbital interaction increases, witnessed by an increase of angle Δ between neighboring quadrupoles and increase in ordering temperature. While the magnetic exchange interaction does not depend much on the moment orientation, this study shows that the quadrupolar interaction depends on the specific orientation of the orbitals and can be manipulated with an applied field.

We thank S.W. Lovesey for valuable discussion. This work was supported by the Swiss National Science Foundation and by a Grant-in-Aid for Scientific Research from the Japan Society for the Promotion of Science. This work was in part performed at the SLS of the Paul Scherrer Institute, Villigen PSI, Switzerland.

¹ S. Grenier, J. P. Hill, D. Gibbs, K. J. Thomas, M.v. Zimmermann, C. S. Nelson, V. Kiryukhin, Y. Tokura, Y. Tomioka, D. Casa, T. Gog, and C. Venkataraman, Phys. Rev. B **69**, 134419 (2004).

² T. Takimoto, Phys. Rev. B **62**, R14641 (2000).

³ P. Morin and D. Schmitt, *Quadrupolar interactions and magneto-eleastic effects in rare earth intermetallic compounds* (Elsevier Science Publishers B.V., 1990), vol. 5 of *Ferromagnetic Materials*, chap. 1, pp. 2–132.

⁴ A. Kiss and P. Fazekas, Phys. Rev. B **71**, 054415 (2005).

⁵ K. Kaneko, H. Onodera, H. Yamauchi, T. Sakon, M. Motokawa, and Y. Yamaguchi, Phys. Rev. B **68**, 012401 (2003).

⁶ Y. Tanaka, T. Inami, T. Nakamura, H. Yamauchi, H. Onodera, K. Ohoyama, and Y. Yamaguchi, J. Phys.: Condens. Matter **11**, L505 (1999).

⁷ K. Hirota, N. Oumi, T. Matsumura, H. Nakao, Y. Wakabayashi, Y. Murakami, and Y. Endoh, Phys. Rev. Lett. **84**, 2706 (2000).

⁸ A. M. Mulders, U. Staub, V. Scagnoli, S. W. Lovesey, E. Balcar, T. Nakamura, A. Kikkawa, G. van der Laan, and J. M. Tonnerre (unpublished).

⁹ U. Staub, A. M. Mulders, O. Zaharko, S. Janssen, T. Nakamura, and S. W. Lovesey, Phys. Rev. Lett. **94**, 036408

(2005).

¹⁰ Y. Tanaka, U. Staub, K. Katsumata, S. W. Lovesey, J. E. Lorenzo, Y. Narumi, V. Scagnoli, S. Shimomura, Y. Tabata, Y. Onuki, et al., Europhys. Lett. **68**, 671 (2004).

¹¹ K. Kaneko, S. Katano, M. Matsuda, K. Ohoyama, H. Onodera, and Y. Yamaguchi, Appl. Phys. A **74**, S1749 (2002).

¹² D. Okuyama, T. Matsumura, H. Nakao, Y. Murakami, H. Onodera, A. Tobe, Y. Wakabayashi, and H. Sawa, J. Phys. Soc. Jpn. **74**, 1566 (2005).

¹³ A. M. Mulders, U. Staub, V. Scagnoli, T. Nakamura, and A. Kikkawa, Physica B (in press).

¹⁴ H. Adachi, H. Kawata, M. Mizumaki, T. Akao, M. Sato, N. Ikeda, Y. Tanaka, and H. Miwa, Phys. Rev. Lett. **89**, 206401 (2002).

¹⁵ S. W. Lovesey, E. Balcar, K. S. Knight, and J. Fernández-Rodríguez, Phys. Rep. **411**, 233 (2005).

¹⁶ K. Kaneko, H. Onodera, H. Yamauchi, K. Ohoyama, A. Tobe, and Y. Yamaguchi, J. Phys. Soc. Jpn. **70**, 3112 (2001).

¹⁷ M. Maino, A. Tobe, and H. Onodera, J. Phys. Soc. Jpn. **74**, 1838 (2005).